Comparison of Dynamic Contrast-Enhanced Gradient-Echo and Spin-Echo Sequences in MR of Head and Neck Neoplasms

Edward J. Escott, Vijay M. Rao, William D. Ko, and Juan E. Guitierrez

PURPOSE: To investigate the utility of dynamic contrast-enhanced gradient-echo MR imaging of head and neck lesions and to compare this technique with the commonly used spin-echo contrast-enhanced fat-saturation technique. **METHODS:** Twenty-two patients with a total of 23 head and neck neoplasms underwent dynamic gradient-echo and spin-echo MR imaging studies. The spin-echo and dynamic gradient-echo images were compared in each case by consensus of three observers for differences in tumor conspicuity and delineation of margins, particularly with regard to invasion of adjacent structures. When possible, pathologic and/or surgical confirmation of tumor extent was obtained. Relative contrast was also calculated to determine objectively the degree of tumor enhancement with respect to background mucosa. **RESULTS:** The dynamic gradient-echo images showed better or equal delineation of the tumor margins by subjective observation in all but two cases. Temporally different enhancement patterns were noted for lesions, background mucosa, and adjacent reaction and edema. The dynamic gradient-echo technique provided better relative contrast than the spin-echo technique in 17 (77%) of 22 lesions. **CONCLUSION:** Dynamic gradient-echo MR imaging is superior to conventional contrast-enhanced spin-echo imaging in delineating the margins and extent of tumor. This technique provided observers with added confidence in their interpretations and suffered from fewer technical limitations.

Index terms: Magnetic resonance, comparative studies; Neck, neoplasms

Accurate assessment of tumor margins and extent of invasion of adjacent structures is essential for proper staging and therapy. Standard spin-echo magnetic resonance (MR) sequences without contrast administration followed by contrast enhancement and fat saturation are commonly used techniques to evaluate head and neck neoplasms. However, these sequences might not accurately define tumor extent because of enhancement of surrounding inflammatory changes or edema or because of the physiological enhancement of normal mucosa and other structures, such as the tongue. Additionally, the lesion might not be evident or can appear smaller if obscured by the physiological enhancement of background tissues.

The use of contrast material in the evaluation of head and neck tumors has been established, particularly with regard to delineation of tumor margins (1). However, an enhanced tumor is difficult to distinguish from surrounding hyperintense fat, a problem that some authors have attempted to resolve with subtraction techniques (1). Lesion enhancement is also commonly distinguished from fat by the use of fat-saturation spin-echo imaging, but there are inherent technical problems with this technique, including inhomogeneous fat saturation and water saturation. Additionally, distinguishing tumor from normally enhancing mucosa can be difficult or impossible.

The use of dynamic enhancement to differentiate tumor from adjacent physiologically enhancing tissues has been discussed with regard to the pituitary gland (2, 3). Previous authors

TABLE 1: Lesion and preferred imaging technique in 23 patients with head and neck tumors

Case	Biopsy Finding	Technique Preferred by Consensus of Three Observers
1	Squamous cell carcinoma	Dynamic
2	Squamous cell carcinoma	Dynamic
3	Rhabdomyoma	Dynamic
4	Small-cell metastasis	Dynamic
5	Squamous cell carcinoma	Dynamic
6	Squamous cell carcinoma	Dynamic
7	Hemangioma	Spin-echo
8	Metastatic melanoma	Dynamic/spin-echo equally
9	Squamous cell carcinoma	Dynamic
10	No recent biopsy, prior hemangioma	Dynamic
11	Granulation tissue, chronic inflammation, treated squamous cell carcinoma	Dynamic
12	Multinodular goiter; hypercellular parathyroid, consistent with adenoma	Dynamic
13	Squamous cell carcinoma, nodal metastasis	Dynamic
14	Recurrent squamous cell carcinoma	Dynamic
15	Squamous cell carcinoma	Dynamic
16	Warthin tumor	Dynamic/spin-echo equally
17	Squamous cell carcinoma	Dynamic
18	Metastatic malignant melanoma	Dynamic/spin-echo equally
19	Squamous cell carcinoma	Dynamic
20	Malignant melanoma	Dynamic/spin-echo equally
21	Squamous cell carcinoma	Spin-echo
22	Squamous cell carcinoma	Dynamic
23	No biopsy	Dynamic

have evaluated the use of dynamic enhancement curves as a method to differentiate benign from malignant neoplasms in the head and neck region, although the success of this method has been questioned by others (4, 5). The issue of whether this technique has true value in delineating tumor margins and in separating tumor from adjacent physiologically and reactively enhancing tissues has been mentioned in the German literature (6). The purpose of this study was to compare dynamic contrast-enhanced gradient-echo MR imaging and fat-saturated contrast-enhanced spin-echo MR imaging in terms of lesion conspicuity and delineation.

Materials and Methods

Twenty-two patients with a total of 23 head and neck neoplasms underwent dynamic gradient-echo and spin-echo MR imaging studies between May 1995 and February 1996. The lesions studied included 11 squamous cell carcinomas, one presumed recurrence of squamous cell carcinoma, one case of granulation tissue (treated squamous cell carcinoma), three malignant melanomas, one hemangioma, one primary salivary gland neoplasm, one rhabdomyoma, one small-cell metastasis, one multinodular goiter with parathyroid adenoma, and two lesions for which biopsies have not yet been done (Table 1). An

additional patient with a supraclavicular neoplasm had dynamic imaging but was not included in the study owing to the location of the lesion.

Our imaging protocol for head and neck tumors included sagittal and axial T1-weighted noncontrast spin-echo sequences, axial short-tau inversion-recovery (STIR) sequences, axial and coronal T1-weighted contrast-enhanced spin-echo sequences with fat saturation, and dynamic contrast-enhanced axial fast multiplanar spoiled gradient-echo (FMPSPGR) sequences with fat saturation. All images were obtained on 1.5-T MR units. The contrast agent was 0.1 mmol/kg gadopentetate dimeglumine. An initial noncontrast FMPSPGR imaging sequence was performed, and the dynamic sequence was begun during the injection of 10 mL of saline flush. This was accomplished by starting an intravenous line before the procedure and using a length of connecting tubing sufficient to allow injection while the patient remained in the scanner. A saline drip was used to keep the intravenous line patent. After the noncontrast FMPSPGR sequence, contrast material was injected via a port in the connecting tubing without moving the patient. The contrast agent was injected by hand at approximately 1 mL/s and the scan was begun during the injection of saline flush. The duration of the initial scan was approximately 30 to 40 seconds (depending on the number of sections and the repetition time), and the subsequent passes were performed consecutively, without interval delay. Therefore, the start times for each of the first three passes were at approximately 0 seconds, 30 to 40 seconds, 60 to 80 seconds, and, if a fourth pass was

TABLE 2: Subjective evaluation of the dynamic technique versus the spin-echo technique

Parameter	Dynamic Gradient-Echo Better than Spin-Echo	Dynamic Gradient-Echo Equal to Spin-Echo	Spin-Echo Better than Dynamic Gradient-Echo
Enhancement	15	4	4
Margins	19	2	2
Overall certainty	17	4	2

obtained, 90 to 120 seconds after injection of the saline flush. A brief (few seconds) delay was allowed between the first and second passes to enable the person injecting the contrast material to leave the scan room.

The specific parameters for the dynamic gradient-echo series included two-dimensional FMPSPGR with a repetition time (TR) of at least 230 milliseconds, which was extended if additional sections were needed, the minimum allowable echo time (TE) (usually 2 to 4 milliseconds), one excitation, 90° flip angle, 20-cm field of view, 256 × 128 matrix, 32-kHz bandwidth, and fat saturation. The section thickness was generally 4 mm, with a 1-mm intersection gap, although this occasionally varied depending on lesion size. A few of the initial scans were done with a shorter TR. Two to four (generally three) consecutive contrast-enhanced sequences were performed. The dynamic technique was, by necessity, always performed before the contrast-enhanced T1-weighted spin-echo fat-saturation axial and coronal images were obtained.

The parameters for the T1-weighted fat-saturation spin-echo technique were 400–583/10–14/2 (TR/TE/excitations), 20-cm field of view, 256 × 128 matrix, 16-kHz bandwidth, and fat saturation. The section thickness was 4 mm, with a 1-mm intersection gap, although this occasionally varied depending on lesion size.

The scan times for the gradient-echo sequence were generally between 30 and 40 seconds, but was occasionally increased for a greater number of sections. The scan times for the spin-echo sequence were generally between 4½ and 6 minutes. For the dynamic gradient-echo scans with the shortest scan time of 32 to 33 seconds, 17 to 19 sections were obtained. For the spin-echo sequences up to 6 minutes in length, 18 to 23 sections were obtained. Both sequences could have additional sections with increased scan time. The number of sections with both techniques was adequate for lesion and neck coverage. The comparable spin-echo and gradient-echo sequences were generally performed with similar section thicknesses, intersection gaps, and areas covered. Overall, the section thickness did not differ by more than 1 mm between techniques, and all scans adequately covered the entire extent of the lesion.

The spin-echo and dynamic gradient-echo images were compared in each case by consensus of three observers (two senior neuroradiology fellows and a senior head and neck radiologist) for differences in tumor conspicuity and delineation of margins, particularly with regard to invasion of adjacent structures. Pathologic diagnosis of tumor type was obtained in 20 of the 23 lesions. When possible, pathologic and/or surgical confirmation of tumor extent

and margins was obtained. However, not all patients underwent total excision or exploration, and treatment was instituted on the basis of biopsy and imaging findings. Surgical/clinical and/or pathologic correlation of lesion extent was obtained in 13 cases. Contrast-to-noise ratios ([signal intensity of lesion − signal intensity of background mucosa]/[standard deviation of background mucosa signal]) and relative contrast ([signal intensity of lesion − signal intensity of background mucosa]/[signal intensity of background mucosa]) were also determined for the contrast-enhanced spin-echo sequences and for each of the dynamic gradient-echo contrast-enhanced passes to determine objectively the degree of tumor enhancement with respect to adjacent normal mucosa evident with each technique.

Results

Subjective Observation

For all but two studies, the observers' certainty in determining the extent of tumor based on degree of enhancement and definition of margins was better or equal with the gradient-echo technique than with the spin-echo technique (Table 2). Among the other two studies, one was a hemangioma (case 7), which, owing to delayed enhancement of portions of this lesion, did not enhance on the gradient-echo series. If the dynamic gradient-echo sequence had been the only series done, and the case monitored, additional dynamic and delayed sequences could have been performed. Nonetheless, the dynamic technique offered a clue to the histology of the lesion, since the filling in pattern seen was typical of a hemangioma (7). In the other study, which was of a squamous cell carcinoma of the tongue (case 21), the images were obtained in a coronal plane, and less susceptibility artifact was seen with the spin-echo technique.

It was generally the first and second passes of the gradient-echo sequence that provided the best lesion conspicuity with respect to background mucosa and adjacent muscle. On the later passes, the images more closely resembled the patterns of enhancement seen on the
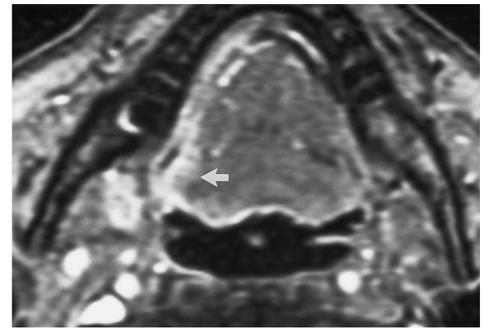
Fig 1. Case 22: squamous cell carcinoma of the tongue.

A, On T1-weighted contrast-enhanced fat-saturation spin-echo image (450/10/2), lesion (*arrow*) in the lateral aspect of the tongue is not seen well.

B, On first pass of dynamic gradient-echo sequence (230/3.1/1), the lesion (*arrow*) is moderately enhancing with respect to the tongue.
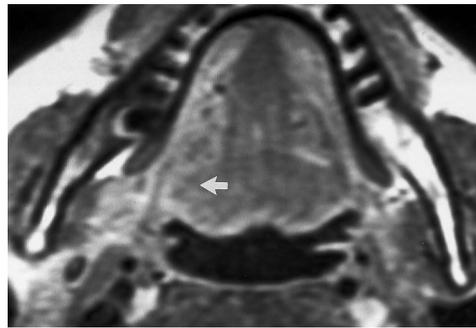

A **B**

Fig 2. Case 11: granulation tissue and inflammatory tissue at site of prior squamous cell carcinoma.

A, T1-weighted contrast-enhanced fat-saturation spin-echo image (400/10/2) shows questionable enhancement at left side of tongue base (*arrows*).

B, On first pass of dynamic gradient-echo sequence (230/3.1/1), definite enhancement is seen at left side of tongue base (*arrows*). At surgery, this proved to be granulation tissue, inflammation, and fibrosis in the location of previously treated squamous cell carcinoma.
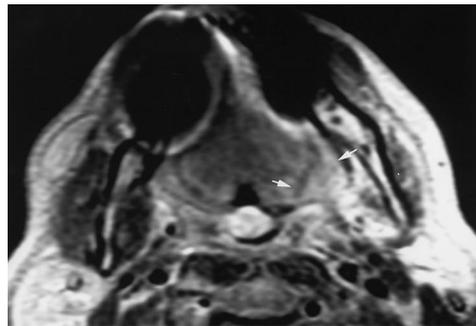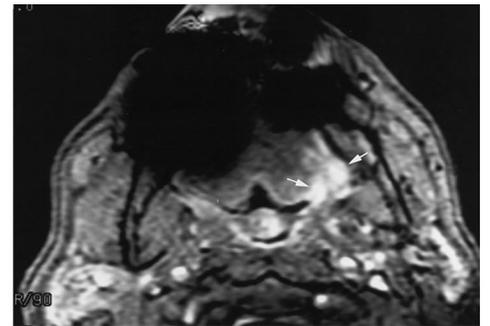

A **B**

Fig 3. Case 14: presumed recurrent squamous cell carcinoma.

A, On T1-weighted contrast-enhanced fat-saturation spin-echo image (533/10/1), no enhancement is seen in the area of suspected recurrence (*straight arrow*).

B, On second pass of dynamic gradient-echo sequence (300/3.1/1), a distinctly enhancing lesion is seen in the area of suspected recurrence (*straight arrow*). This was presumed to represent recurrence clinically as well, and was treated. Note the necrotic, metastatic node (*curved arrows* in *A* and *B*).
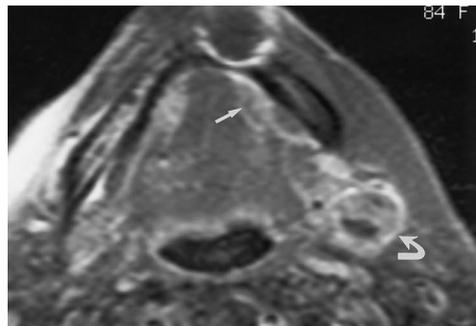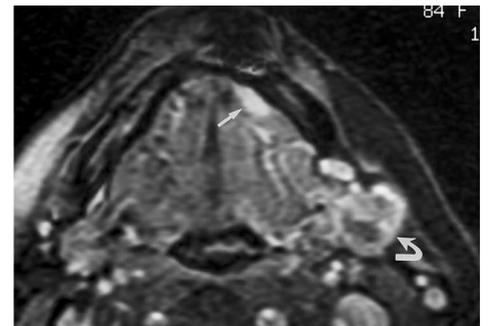
A **B**

spin-echo sequences; in particular, the lesion and background had similar degrees of enhancement.

All lesions depicted with the spin-echo technique were also detected with the gradient-echo technique, although the converse was not true. Three lesions (cases 11, 14, and 22) were definitely detected by the gradient-echo technique only (Figs 1–3). Even in retrospect, these lesions would probably be ascribed to inhomogeneous enhancement on the spin-echo images,

and not reported. A fourth lesion (case 9) was only faintly seen on the spin-echo images (Fig 4). In each of these cases, the lesions involved the tongue. The lack of lesion conspicuity on the spin-echo sequences was mainly due to enhancement of the tongue and to volume averaging with adjacent enhancing structures, such as the sublingual glands.

In the remaining 17 cases, the gradient-echo technique consistently provided increased observer confidence with respect to assessment of
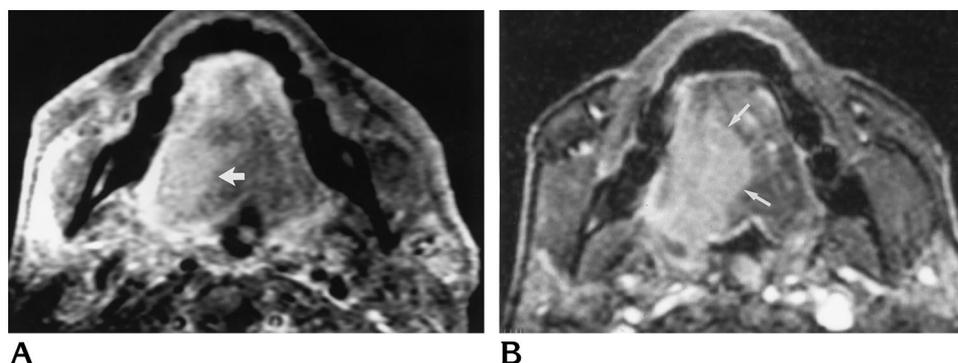
A   B

Fig 4. Case 9: squamous cell carcinoma of the tongue.

A, On T1-weighted contrast-enhanced spin-echo image (500/14/2), lesion (arrow) involving right side of the tongue is mildly enhancing with respect to rest of tongue.

B, On first pass of dynamic gradient-echo sequence (100/3.1/2), the full extent of the lesion (arrows), which now has marked enhancement with respect to rest of tongue, is seen. The extent of the lesion on this sequence corresponded with the surgical extent.

lesion margins, absence of vascular invasion or occlusion, and lesion extent. It was these factors that gave the observers greater overall confidence in the gradient-echo technique despite the fact that degree of enhancement was equal to or less than that of the spin-echo technique in eight cases. The first and second passes of the dynamic studies best showed the lesion extent, because of increased lesion conspicuity with respect to background mucosa. Additionally, fat saturation was generally more uniform and more complete with the gradient-echo technique than with the spin-echo technique. In general, the susceptibility artifacts on the gradient-echo sequences did not significantly degrade image quality, and sections were obtained to minimize this effect. Owing to the short TE on the gradient-echo sequences (2 to 4 milliseconds), susceptibility artifacts were not that much greater than on the spin-echo sequences.

The vascular flow-related enhancement on the gradient-echo images was judged beneficial in identifying the vascular structures and in assessing vascular invasion. Additionally, this vascular flow-related enhancement could potentially help to differentiate normal vessels from enhancing tumor extending through the foramen. In case 2, the venous structures extending through the hypoglossal canals had greater signal on the gradient-echo images than on the corresponding spin-echo images with respect to adjacent nasopharyngeal carcinoma. On the gradient-echo images, vessel margins were consistently seen more clearly with respect to enhancing tumor and vessel patency and displacement could also be better assessed.
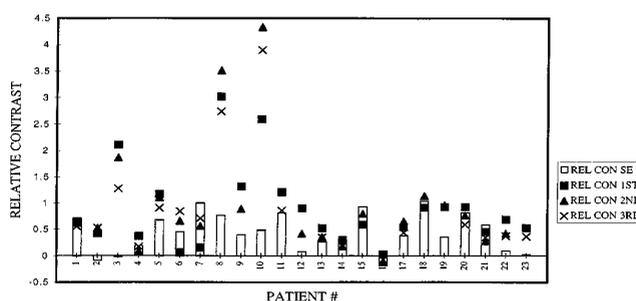

Fig 5. Relative contrast for the spin-echo images and the three dynamic passes for each patient. REL CON SE indicates relative contrast for the spin-echo images; REL CON 1ST, 2ND, 3RD, relative contrast for each of the three dynamic passes.

Contrast-to-Noise Ratio and Relative Contrast

One lesion (a parotid Warthin tumor, case 16) is not included in the figures because it had less enhancement than background with both techniques. Two other lesions (cases 2 and 3) that also had negative relative contrast values (less lesion enhancement than background mucosa enhancement) with the spin-echo technique had positive contrast values with the gradient-echo technique, so they are included. In 16 of 22 cases, the contrast-to-noise ratio was greater with the first or second pass of the dynamic gradient-echo technique than with the spin-echo technique. Seventeen of 22 lesions showed better relative contrast with the gradient-echo technique (Fig 5). In case 14 (Fig 3), the region in which the lesion was located had higher relative contrast on the spin-echo images than on the gradient-echo images, even though the observers could not identify the lesion on the spin-echo sequences. The increased relative contrast was probably due to volume

averaging with the enhancing sublingual gland, which was adjacent to the lesion.

Discussion

Tissue enhancement is dependent on several factors, including vascularity, capillary permeability, renal clearance, and extracellular fluid composition and volume (8–13). Dynamic MR imaging works by capitalizing on the different temporal enhancement characteristics of tissues caused by differences in these factors, enabling differential enhancement between tumors and adjacent physiologically enhancing tissues, and possibly between surrounding edema and inflammation (8, 10–12, 14, 15). For example, there is significant enhancement of the intrinsic tongue muscles, and all structures rich in vascularity, such as the pharyngeal mucosa, as well as many neoplasms (1). All these structures may appear similar on conventional contrast-enhanced MR images, which require an imaging time of a number of minutes. The dynamic technique is better able to differentiate these structures from neoplasm, allowing the investigator to determine the true extent of a lesion.

Contrast-enhanced imaging has been shown to be more sensitive in detecting lesions of the head and neck than is either noncontrast T1- or T2-weighted imaging alone, although not better than these sequences combined (4). The true benefit of contrast-enhanced imaging is in better lesion delineation and better estimation of lesion size, as well as better definition of normal anatomic structures (1). Initial problems with differentiating enhancing lesions from hyperintense fat have been surmounted with the use of fat-saturation techniques. However, differentiation of enhancing masses from normally enhancing structures needs to be overcome to truly evaluate lesion extent.

The current availability of fast scanning techniques makes the acquisition of multiple sequences immediately after administration of contrast material possible. With the FMPSPGR technique, we were able to obtain a series with adequate signal that covered most lesions of the head and neck in approximately 30 seconds. This rapid scanning enabled multiple sequences to be obtained during the phases of lesion and background enhancement that otherwise would occur during the single contrast-enhanced spin-echo fat-saturation sequence.

This dynamic technique therefore enabled us to differentiate lesions from background tissues by their different enhancement characteristics. In the majority of cases in our series, lesion enhancement was greater than that of background tissue (tongue and mucosa) on the initial sequences. Therefore, lesion extent could be better determined on the earlier phases of the dynamic sequence. The delayed gradient-echo sequences were similar to the spin-echo images, as the contrast enhancement reached an equilibrium for all tissues and the differential enhancement characteristics could not be taken advantage of. It was helpful to perform multiple passes, as this ensured obtaining the optimal differentiation between lesion and background, and helped overcome such variables as differences in injection times and circulation rates. These multiple passes do not significantly increase scanning time, as up to four passes can be completed in approximately 2 to 3 minutes, depending on the number of sections obtained.

In four patients (cases 9, 11, 14, and 22), lesions were seen poorly on the spin-echo sequences, and, without the benefit of additional sequences, could have been missed (Figs 1–4). This was caused by obscuration of the lesion by the physiological enhancement of adjacent tissues (cases 9, 11, and 14,) or by subtle, nonuniform enhancement of the lesion (case 22). Each of these lesions was seen distinctly on the gradient-echo images. The relative contrast was greatest for the first pass of the gradient-echo sequence, further indicating that the lesions were obscured by the background tongue enhancement on subsequent passes and on the longer spin-echo sequence. Our subjective evaluation yielded similar results to the objective findings; however, in one patient (case 14), the second pass was preferred.

Although pathologic or surgical confirmation of lesion margins was not available in all cases, we had some evidence that the spin-echo technique overestimated lesion extent as a result of enhancement of adjacent reaction and/or edema and mucosa (cases 1, 3, 6, 15, 17, and 23) (Figs 6 and 7). The enhancement of edema and surrounding reaction on delayed images has been noted with treated osteosarcomas (14). In some of these cases, this perilesional enhancement was assumed, as the lesion boundaries became progressively less distinct with time and on the spin-echo images. In case 3 particularly, it was difficult to separate the

A

B
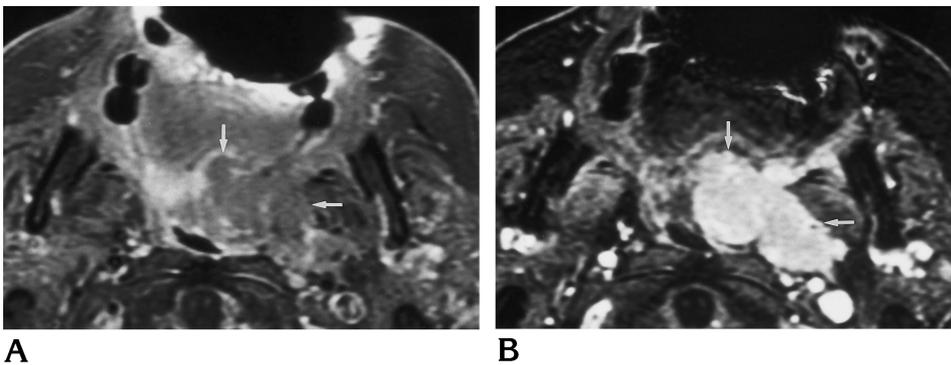
A

B

Fig 6. Case 3, rhabdomyoma.

A, On T1-weighted contrast-enhanced spin-echo image (400/14/2), the mass involving the left side of the pharynx is seen mainly because of its size and the distortion of surrounding architecture, but the margins are not well defined (*arrows*).

B, On first pass of dynamic gradient-echo sequence (230/3.1/1), the lesion is now markedly enhancing with respect to the adjacent tissues, and the full extent of the lesion and its margins are seen (*arrows*).
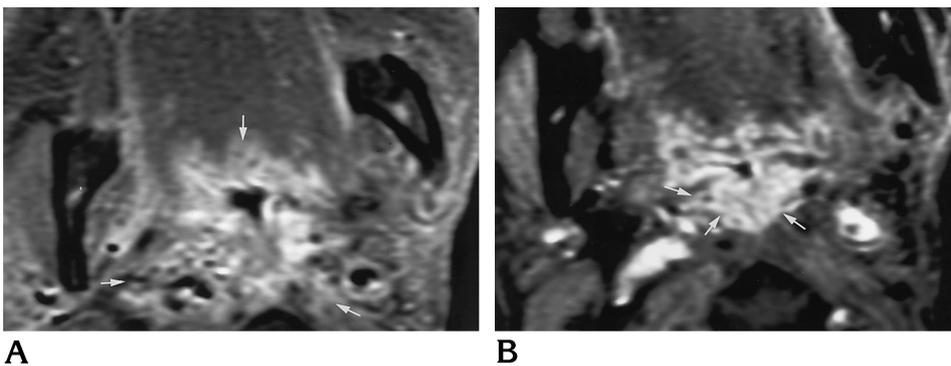
Fig 7. Case 15, recurrent squamous cell carcinoma.

A, On T1-weighted contrast-enhanced spin-echo image (533/10/2), the lesion's margins (*arrows*) are indistinct and its extent is difficult to define, as subtle enhancement involves an extensive area, owing to presumed enhancement of surrounding reaction or edema.

B, On first pass of dynamic gradient-echo sequence (310/2.9/1), the lesion's margins (*arrows*) are sharply defined, possibly due to the neoplasm enhancing before the surrounding reaction.

lesion from adjacent structures on the spin-echo images owing to similar enhancement of lesion and background. However, the lesion's boundaries were clearly evident because of pronounced enhancement on the gradient-echo images, best seen on the first pass (Fig 6). In cases 6 and 15, the lesions' margins became less distinct on the spin-echo images (Fig 7); and in case 1, separation between the lesion and the submandibular gland and carotid sheath became less distinct. At surgery, these adjacent structures were not involved by tumor.

In one patient (case 23), the later gradient-echo images and the spin-echo images showed enhancement extending into the submandibular space and apparently increased thickness of the lesion wall. Because this lesion has not been resected, no pathologic confirmation is available as to whether this additional enhancement was reactive or neoplastic. Since this lesion most likely represents a predominantly cystic lymphangioma, with the majority of the lesion located lateral to the mandible, we suspect it is reactive on the basis of our experience with the other cases.

The benefits of the gradient-echo technique were not as evident in the cases of parotid lesions and melanoma. In these cases, delineation of lesion margin and enhancement with the gradient-echo technique were equal to or better than with the spin-echo technique. The parotid lesion (case 16) was less enhancing than its adjacent gland, and therefore did not benefit from the dynamic technique, since it was the lack of enhancement that made it apparent. This lesion was judged to be equally well seen with both techniques, and therefore nothing would have been lost if only the gradient-echo technique had been performed (Fig 8). One of the three melanomas was hyperintense before contrast administration (case 20) and one, located in the parotid gland (case 18), was seen better before contrast administration. The third was located in the subcutaneous fat of the posterior part of the neck (case 8) and therefore was clearly identified on both sequences. However, the margins of this lesion were judged to be more distinct on the gradient-echo images, mainly because of better suppression of fat. This combined effect of frequency-selective fat

Fig 8. Case 5: Warthin tumor. On T1-weighted contrast-enhanced spin-echo image (533/10/2) (*A*), the right parotid mass (*arrow*) is less enhancing than the surrounding gland, but equally well seen on the second pass of the dynamic gradient-echo sequence (230/2.9/1) (*B*). Therefore, the lesion would have been identified even if just the dynamic sequence had been performed.

A   **B**
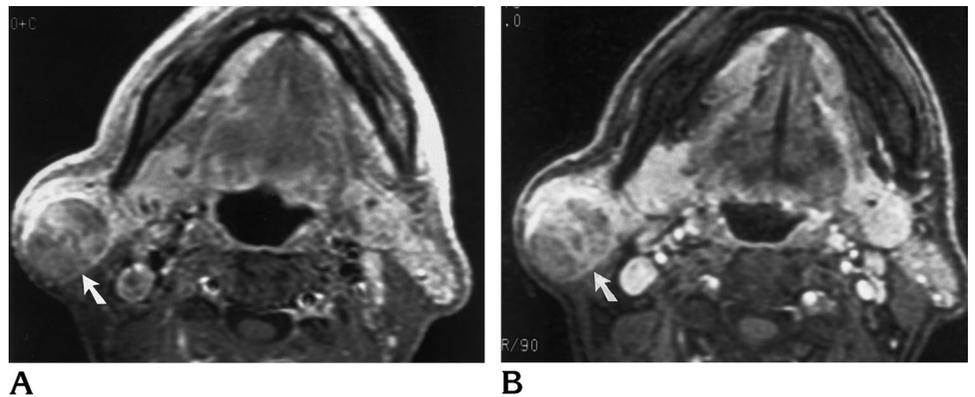
saturation and short-TE FMPSPGR imaging has been shown to provide effective fat saturation in the abdomen (16).

Two cases revealed limitations of the technique. In the patient with the supraclavicular lesion, who was not included in the study, the lesion was in an area that would be better evaluated with computed tomography. With the gradient-echo technique, the lesion was difficult to differentiate from normal vessels in this region owing to flow-related enhancement; and with the spin-echo technique, the lesion was difficult to differentiate from surrounding tissues owing to inhomogeneous fat saturation. The STIR images actually provided the most information. For one of the patients with a tongue lesion (case 21), the dynamic study was obtained in the coronal plane, with suboptimal visualization of the lesion. Although susceptibility artifacts from dental hardware severely limited the gradient-echo sequence, the lesion could still be seen; however, the artifact limited the observers' confidence in defining the lesion's margins. It is possible, however, that the lesion was more conspicuous on the spin-echo images, since its size was overestimated owing to enhancement of adjacent tissue resulting from inflammation and edema.

One patient (case 11, Fig 2) had only granulation tissue and changes associated with radiation necrosis found at surgery in an area of previously treated squamous cell carcinoma. No tumor was found in the area that appeared abnormal at imaging. This represented a false-positive case for the gradient-echo technique, but demonstrated its sensitivity, since the lesion was not seen on the spin-echo images.

Overall, if a single contrast-enhanced technique is to be used, the dynamic gradient-echo technique has many advantages over the spin-

echo technique. Subjectively, the gradient-echo technique was preferred by the observers over the spin-echo technique in the majority of cases. The standard measurements of lesion conspicuity (the contrast-to-noise ratio and the relative contrast) differed somewhat from the subjective evaluation, as the features the observers found most favorable with the gradient-echo technique were not reflected in these numbers. These features include better definition of lesion margins, better delineation from adjacent structures, and better and more homogeneous fat saturation. So, although the lesions were often seen with both techniques, the confidence of the observers in defining their extent was superior with the gradient-echo technique.

In conclusion, our study demonstrates that dynamic gradient-echo imaging is superior to conventional contrast-enhanced fat-saturated spin-echo imaging in delineating tumor margins and extent. The former technique suffered from fewer technical limitations and provided the radiologists with added confidence in their interpretation. On the basis of the results of this study, the dynamic gradient-echo technique is routinely used at our institution for evaluation of head and neck neoplasms.

References

1. Vogl T, Dresel S, Juergens M, Assal J, Lissner J. MR imaging with Gd-DTPA in lesions of the head and neck. *J Otolaryngol* 1993; 22:220–230
2. Davis WL, Lee JN, King BD, Harnsberger HR. Dynamic contrast-enhanced MR imaging of the pituitary gland with fast spin-echo technique. *J Magn Reson Imaging* 1994;4:509–511
3. Kucharzyk W, Bishop JE, Plewes DB, Keller MA, George S. Detection of pituitary microadenomas: comparison of dynamic keyhole fast spin-echo, unenhanced, and conventional contrast-enhanced imaging. *AJR Am J Roentgenol* 1994;163:671–679
4. Takashima S, Noguchi Y, Okumura T, Hideharu A, Tetsuro K.

Dynamic MR imaging in the head and neck. *Radiology* 1993;189:
813–821

5. Yousem DM. Dynamic MR imaging of the head and neck: an idea whose time has come. . . and gone? *Radiology* 1993;189:659–660

6. Maurer VJ, Hellwig A, Matthaei D, Carduck H-P. Erste klinische Erfahrungen mit einer dynamischen FLASH-2D-Sequenz bei tumoren im kopf- und halsbersich. *Fortschr Rontgenstr* 1993;158:451–455

7. Mafee MF, Putterman A, Valvassori GE, et al. Orbital space-occupying lesions: role of computed tomography and magnetic resonance imaging. An analysis of 145 cases. *Radiol Clin North Am* 1987;25:529–559

8. Verstraete KL, Van der Woude HJ, Hogendoorn PCW, Deene YD, Kunnen M, Bloem JL. Dynamic contrast-enhanced MR imaging of musculoskeletal tumors: basic principles and clinical applications. *J Magn Reson Imaging* 1996;6:311–321

9. Brasch RC. New directions in the development of MR imaging contrast media. *Radiology* 1992;183:1–11

10. Som PM, Lanzieri CF, Sacher M, Lawson W, Biller HF. Extracranial tumor vascularity: determination by dynamic CT scanning, 1: concepts and signature curves. *Radiology* 1985;154:401–405

11. Som PM, Lanzieri CF, Scaher M, Lawson W, Biller HF. Extracranial tumor vascularity: determination by dynamic CT scanning, 2: the unit approach. *Radiology* 1985;154:407–412

12. Michael AS, Mafee MF, Valvassori GF, Tan WS. Dynamic computed tomography of the head and neck: differential diagnostic value. *Radiology* 1985;154:413–419

13. Kormano M, Dean PB. Extravascular contrast material: the major component of contrast enhancement. *Radiology* 1976;121:379–382

14. De Baere T, Vanel D, Shapeero LG, Charpentier A, Terrier P, di Paola M. Osteosarcoma after chemotherapy: evaluation with contrast material-enhanced subtraction MR imaging. *Radiology* 1992;185:587–592

15. Reddick WE, Langston JW, Meyer WH, et al. Discrete signal processing of dynamic contrast-enhanced MR imaging: statistical validation and preliminary clinical application. *J Magn Reson Imaging* 1994;4:397–404

16. Siegelman ES, Outwater EK, Vinitski S, Mitchell DG. Fat suppression by saturation/opposed phase hybrid technique: spin echo versus gradient-echo imaging. *Magn Reson Imaging* 1995;13:545–548